

**Chiral approach to phi radiative decays**Deirdre Black,<sup>1,\*</sup> Masayasu Harada,<sup>2,†</sup> and Joseph Schechter<sup>3,‡</sup><sup>1</sup>*Department of Physics, Cavendish Laboratory, University of Cambridge, J. J. Thomson Avenue, Cambridge CB3 0HE, United Kingdom*<sup>2</sup>*Department of Physics, Nagoya University, Nagoya 464-8602, Japan*<sup>3</sup>*Department of Physics, Syracuse University, Syracuse, New York 13244-1130, USA*

(Received 5 January 2006; published 23 March 2006)

The radiative decays of the phi meson are known to be a good source of information about the  $a_0(980)$  and  $f_0(980)$  scalar mesons. We discuss these decays starting from a nonlinear model Lagrangian which maintains the (broken) chiral symmetry for the pseudoscalar (P), scalar (S) and vector (V) nonets involved. The characteristic feature is derivative coupling for the SPP interaction. In an initial approximation which models all the scalar nonet radiative processes together with the help of a pointlike vertex, it is noted that the derivative coupling prevents the  $a_0$  and  $f_0$  resonance peaks from getting washed out (by falling phase space). However, the shapes of the invariant two final PP mass distributions do not agree well with the experimental ones. For improving the situation we verify that inclusion of the charged  $K$  meson loop diagrams in the model does reproduce the experimental spectrum shapes in the resonance region. The derivative coupling introduces quadratic as well as logarithmic divergences in this calculation. Using dimensional regularization we show in detail that these divergences actually cancel out among the four diagrams, as expected from gauge invariance. We point out the features which are expected to be important for further work on this model and for learning more about the puzzling scalar mesons.

DOI: [10.1103/PhysRevD.73.054017](https://doi.org/10.1103/PhysRevD.73.054017)

PACS numbers: 14.40.-n, 11.30.Rd, 12.40.Vv, 13.25.Jx

**I. INTRODUCTION**

Recently, there have been a number of important experimental studies [1] of the rare radiative decays of the  $\phi(1020)$  vector meson:  $\phi \rightarrow \pi\pi\gamma$  and  $\phi \rightarrow \pi\eta\gamma$ . These decays seem to be dominated by the production (and subsequent decay) of the scalar mesons,  $a_0(980)$  and  $f_0(980)$  according to  $\phi \rightarrow f_0, a_0 + \gamma$  and hence are generally considered to provide valuable information about the puzzling light scalar mesons [2] of low energy QCD.

The theoretical analysis of this type of decay was initiated by Achasov and Ivanchenko [3] and followed up by many others [4]. The starting point was the observation that the  $\phi$  meson decays about 50% of the time into  $K^+K^-$ . Since this final state can easily annihilate to produce either an  $f_0$  or  $a_0$  together with an emitted photon, it is rather natural to consider charged  $K$ -meson loop diagrams to describe the process. Similarly the  $\phi$  meson is observed to decay about 15% of the time to  $\pi\rho$  or  $\pi^+\pi^-\pi^0$  so one expects some nonresonant background which is likely to include the emission of a pion with a virtual  $\rho$  which subsequently decays into  $\pi\gamma$  (and similar diagrams leading to a  $\pi^0\eta\gamma$  final state).

The varied calculations along these lines lead to results which more or less agree with experiment. Of course it is desirable to fine-tune this agreement, both to reflect the expected improved accuracy of new experiments as well as

to improve our understanding of strong interaction calculations. Here we will focus on some technical points, which do not much change the previous results but may be of interest for future more ambitious calculations as more experimental data become available. Mainly, we will require that the amplitudes all be computed from a chiral invariant Lagrangian (containing usual quark mass induced breaking terms). This is a symmetry of nature apparently so it is desirable to calculate in this way even though the spontaneous breakdown of chiral symmetry (in the absence of quark mass terms) means that, especially away from thresholds, one can often get reasonable predictions by not explicitly taking it into account.

Two approaches are commonly employed to implement the chiral symmetry in the effective Lagrangian framework. In the linear sigma model approach, scalar partners of the pseudoscalars are introduced. In the nonlinear sigma model approach, one initially deals with pseudoscalars only, the scalars having been essentially “integrated out.” The characteristic feature of the nonlinear model is the appearance of derivative-type interaction terms as opposed to nonderivative-type interaction terms in the linear model. Nevertheless, the nonlinear model is often more convenient to use. For example, the celebrated result [5] for near threshold  $\pi$ - $\pi$  scattering arises in the linear model from a delicate cancellation of two rather large terms. On the other hand it arises directly from a simple single term of the correct characteristic strength in the nonlinear model. In the present paper we shall deal with the nonlinear model approach. Since vector and scalar mesons are also involved in the processes of interest we will add these to the non-

\*Email address: [black@hep.phy.cam.ac.uk](mailto:black@hep.phy.cam.ac.uk)†Email address: [harada@hken.phys.nagoya-u.ac.jp](mailto:harada@hken.phys.nagoya-u.ac.jp)‡Email address: [schechte@physics.syr.edu](mailto:schechte@physics.syr.edu)

linear Lagrangian of pseudoscalars in a conventional way. Such a formulation essentially implements vector meson dominance automatically for processes involving photons.

We shall restrict our attention further here to processes of the type  $\phi \rightarrow \gamma +$  virtual scalar where the virtual scalar (either  $a_0$  or  $f_0$ ) subsequently decays to two pseudoscalars. First we shall consider a possible non- $K^+$  loop contribution to this process. We previously [6] studied this by introducing an effective strong VVS (vector-vector scalar) interaction based on an analogy to the effective VVP (vector-vector pseudoscalar) interaction used many years ago [7] to study analogous processes like  $\omega(782) \rightarrow \pi^0 \gamma$ . This might open the possibility of understanding properties of the whole nonet of scalars at once. Especially, it might shed some light on the composition of the light scalar nonet; whether the light scalar mesons are composed of one quark and one antiquark (2-quark picture) or two quarks and two antiquarks (4-quark picture).

In the present paper, we point out an interesting effect. If a nonderivative SPP-type interaction were to be used there would be a strong tendency for the decreasing phase space to wash out the predicted scalar meson peak in, for example,  $d\Gamma(\phi \rightarrow \pi^0 \eta \gamma)/dq$ . Here  $q^2$  is the invariant squared mass for the  $\pi\eta$  system. On the other hand, the use of a derivative-type SPP interaction, as is required for chiral symmetry in the nonlinear sigma model approach, restores the peak. (There is not necessarily any contradiction with the expectation that the same physics near threshold should be expressed by suitably generalized linear and nonlinear models. One expects the linear model description to include additional terms.) However, we notice that there is experimentally more enhancement of the scalar peak than can be accounted for by this mechanism. Thus we are led to also consider the usual  $K^+$  loop diagram in our approach.

As mentioned, the  $K^+$  loop diagram has been considered by many authors [3,4]. We cannot basically change the well-established results. However we note that the effect of the derivative couplings will also sharpen the scalar peak. Actually, the derivative SPP couplings result in quadratic as well as logarithmic divergences and an additional diagram. It has been found [8] that such ‘‘unpleasant details’’ of the calculation can be circumvented by assuming gauge invariance. Specifically, gauge invariance requires that the amplitude for  $\phi \rightarrow$  photon + scalar be proportional to  $\epsilon_\mu \epsilon_\nu^V (\delta_{\mu\nu} p \cdot k - p_\mu k_\nu)$ , where  $\epsilon^V$  and  $p$  are, respectively, the polarization and momentum four vectors of the  $\phi$  meson while  $\epsilon$  and  $k$  correspond to the photon. Then it is only necessary to calculate the coefficient of the  $p_\mu k_\nu$  term, which eliminates the need to calculate two diagrams and worry about divergences actually canceling each other. Of course it would be nice to regulate all the diagrams and verify in detail how the cancellations take place. We have carried out this somewhat lengthy task using the dimensional regularization scheme and will give details in the present paper.

In Sec. II, we first present the chiral Lagrangian of pseudoscalars, vectors and scalars which will be used for the subsequent calculations. Our initial motivation, described in Ref. [6], was to relate all the decays of the types  $S \rightarrow \gamma\gamma$ ,  $V \rightarrow S\gamma$  and  $S \rightarrow V\gamma$  to each other by using a simple effective pointlike interaction. We next consider the  $\phi(1020)$  decays into  $\pi^0 \eta$  and  $\pi^0 \pi^0$  proceeding, respectively, from intermediate  $a_0(980)$  and  $f_0(980)$  resonances in this simple model. It can be seen that the spectrum shapes for large  $q$  are not as sharply peaked as the experimental data indicate.

In Sec. III, we calculate the form of the charged  $K$  meson loop contributions to these two decays using a nonlinear chiral Lagrangian which maintains the chiral invariance when vectors and scalars as well as pseudoscalars are included. The extension to include photon interactions is given. It is noted that individual diagrams contain quadratic as well as logarithmic divergences. A careful treatment using the dimensional regularization scheme shows that these divergences both cancel leaving a finite answer.

In Sec. IV we study the spectrum shape of the  $K$ -loop contributions to these decays. We find that this has a characteristic shape which does in fact agree with experiment, suggesting that the dynamics of the  $K$ -loop plays an important role.

Section V contains a brief summary. Some discussion will be given on the status of the present program and related future work.

## II. VVS-TYPE CONTRIBUTIONS TO $\phi \rightarrow \pi^0 \eta \gamma$ AND $\phi \rightarrow \pi^0 \pi^0 \gamma$

Our calculation is based on a standard nonlinear chiral Lagrangian containing, in addition to the pseudoscalar nonet matrix field  $\phi$ , the vector meson nonet matrix  $\rho_\mu$  and a scalar nonet matrix field denoted by  $N$ . Under chiral unitary transformations of the three light quarks,  $q_{L,R} \rightarrow U_{L,R} \cdot q_{L,R}$ , the chiral matrix  $U = \exp(2i\phi/F_\pi)$ , where  $F_\pi \simeq 0.131$  GeV, transforms as  $U \rightarrow U_L \cdot U \cdot U_R^\dagger$ . The convenient matrix  $K(U_L, U_R, \phi)$  [9] is defined by the following transformation property of  $\xi$  ( $U = \xi^2$ ):  $\xi \rightarrow U_L \cdot \xi \cdot K^\dagger = K \cdot \xi \cdot U_R^\dagger$ , and specifies the transformations of ‘‘constituent-type’’ objects. The fields we need transform as

$$\begin{aligned} N &\rightarrow K \cdot N \cdot K^\dagger, & \rho_\mu &\rightarrow K \cdot \rho_\mu \cdot K^\dagger + \frac{i}{\tilde{g}} K \cdot \partial_\mu K^\dagger, \\ F_{\mu\nu}(\rho) &= \partial_\mu \rho_\nu - \partial_\nu \rho_\mu - i\tilde{g}[\rho_\mu, \rho_\nu] \rightarrow K \cdot F_{\mu\nu} \cdot K^\dagger, \end{aligned} \quad (2.1)$$

where the coupling constant  $\tilde{g}$  is about 4.04. One may refer to Ref. [10] for our treatment of the pseudoscalar-vector Lagrangian and to Ref. [11] for the scalar addition. The

entire Lagrangian is chiral invariant (modulo the quark mass term induced symmetry breaking pieces) and, when electromagnetism is added, gauge invariant. The  $U(3)_L \times U(3)_R$  invariant portion of the effective Lagrangian reads<sup>1</sup>

$$\begin{aligned} \mathcal{L}_0 = & -\frac{F_\pi^2}{2} \text{Tr}(p_\mu p_\mu) - \frac{1}{4} \text{Tr}(F_{\mu\nu}(\rho) F_{\mu\nu}(\rho)) - \frac{1}{2} \text{Tr}(\mathcal{D}_\mu N \mathcal{D}_\mu N) - \frac{m_v^2}{2\tilde{g}^2} \text{Tr}[(\tilde{g}\rho_\mu - v_\mu)^2] - a \text{Tr}(NN) \\ & - c \text{Tr}(N) \text{Tr}(N) + F_\pi^2 [A \epsilon^{abc} \epsilon_{def} N_a^d (p_\mu)_b^e (p_\mu)_c^f + B \text{Tr}(N) \text{Tr}(p_\mu p_\mu) + C \text{Tr}(N p_\mu) \text{Tr}(p_\mu) \\ & + D \text{Tr}(N) \text{Tr}(p_\mu) \text{Tr}(p_\mu)], \end{aligned} \quad (2.2)$$

where  $\mathcal{D}_\mu N = \partial_\mu N - i\tilde{g}\rho_\mu N + iN\tilde{g}\rho_\mu$ .<sup>2</sup> Furthermore  $v_\mu, p_\mu = (i/2)(\xi\partial_\mu\xi^\dagger \pm \xi^\dagger\partial_\mu\xi)$ , where  $\xi = U^{1/2}$ . These terms include the parameters  $m_v^2, a, c, A, B, C$  and  $D$ . More details about the evaluation of these parameters are discussed in Refs. [10,16].

It should be remarked that the effect of adding vectors to the chiral Lagrangian of pseudoscalars only is to replace the photon coupling to the charged pseudoscalars as

$$\begin{aligned} ie\mathcal{A}_\mu \text{Tr}(Q\phi\vec{\partial}_\mu\phi) \rightarrow e\mathcal{A}_\mu \left[ k\tilde{g}F_\pi^2 \text{Tr}(Q\rho_\mu) \right. \\ \left. + i\left(1 - \frac{k}{2}\right) \text{Tr}(Q\phi\vec{\partial}_\mu\phi) \right] + \dots, \end{aligned} \quad (2.3)$$

where  $\mathcal{A}_\mu$  is the photon field,  $Q = \text{diag}(2/3, -1/3, -1/3)$  and  $k = (m_v/\tilde{g}F_\pi)^2$  with  $m_v \simeq 0.76$  GeV. The ellipsis stands for symmetry breaking corrections. We see that in this model, Sakurai's vector meson dominance [17] simply amounts to the statement that  $k = 2$  (the KSRF relation [18]). This is a reasonable numerical approximation which is essentially stable to the addition of symmetry breakers [10,19] and we employ it here by neglecting the last term in Eq. (2.3).

The proposed effective SVV-type terms in the effective Lagrangian are [6]:

<sup>1</sup>This Lagrangian can be rewritten within the framework of the hidden local symmetry (HLS) [12,13]. The method of including vector mesons used in this paper based on the proposal in Ref. [14] is equivalent to that based on the HLS approach at tree level [15]. When we consider the vector mesons inside the loop, the two approaches might have some differences. In the present analysis, however, we will consider the loop corrections from only the kaon, which provides a large enhancement to the  $\phi$  radiative decay amplitude. All other loop corrections from vector mesons are naturally expected to be small. In this sense, the method used in this paper is completely equivalent to the recently developed method [13] used in the HLS. Note that the scalar mesons have not been included inside the loop in either approach.

<sup>2</sup>One could also use for the covariant derivative, the combination  $c\tilde{g}\rho_\mu + (1-c)v_\mu$  with  $c$  being an arbitrary constant. In any case, there are a few more terms such as  $\text{Tr}((\tilde{g}\rho_\mu - v_\mu)N(\tilde{g}\rho_\mu - v_\mu)N)$  and  $\text{Tr}((\tilde{g}\rho_\mu - v_\mu)^2 N^2)$ , which include the same number of derivatives. We note that the above extra terms as well as the interaction terms from the covariant derivative do not contribute in the present analysis, where we are considering the processes related to only one scalar meson.

$$\begin{aligned} \mathcal{L}_{\text{SVV}} = & \beta_A \epsilon_{abc} \epsilon^{a'b'c'} [F_{\mu\nu}(\rho)]_a^b [F_{\mu\nu}(\rho)]_{b'}^{c'} \\ & + \beta_B \text{Tr}[N] \text{Tr}[F_{\mu\nu}(\rho) F_{\mu\nu}(\rho)] \\ & + \beta_C \text{Tr}[N F_{\mu\nu}(\rho)] \text{Tr}[F_{\mu\nu}(\rho)] \\ & + \beta_D \text{Tr}[N] \text{Tr}[F_{\mu\nu}(\rho)] \text{Tr}[F_{\mu\nu}(\rho)]. \end{aligned} \quad (2.4)$$

Chiral invariance is evident from Eq. (2.1) and the four flavor invariants are needed for generality. [A term  $\sim \text{Tr}(FFN)$  is linearly dependent on the four shown.] Actually the  $\beta_D$  term does not contribute in our model so there are only three relevant parameters  $\beta_A, \beta_B$  and  $\beta_C$ .

### A. $a_0(980)$ production

The Feynman diagram for the contribution from the new VVS terms to the decay process  $\phi(p, \epsilon^V) \rightarrow \pi^0(q_1)\eta(q_2)\gamma(k, \epsilon)$  is shown in Fig. 1. Note that the photon is produced through its mixing with vector mesons according to Eq. (2.3). The Feynman amplitude is

$$e(q_1 \cdot q_2) Y_{a_0}^{(\pi\eta)} [(p \cdot k)(\epsilon^V \cdot \epsilon) - (p \cdot \epsilon)(k \cdot \epsilon^V)], \quad (2.5)$$

where

$$Y_{a_0}^{(\pi\eta)} = \frac{C_\phi^{a_0}}{\tilde{g}} D_{a_0}(q^2) \gamma_{a_0\pi\eta}. \quad (2.6)$$

Here  $C_\phi^{a_0}$  is given in terms of the coefficients of Eq. (2.4) and a scalar mixing angle in Eq. (8) of Ref. [6] and will be considered, for generality, a single parameter. Furthermore

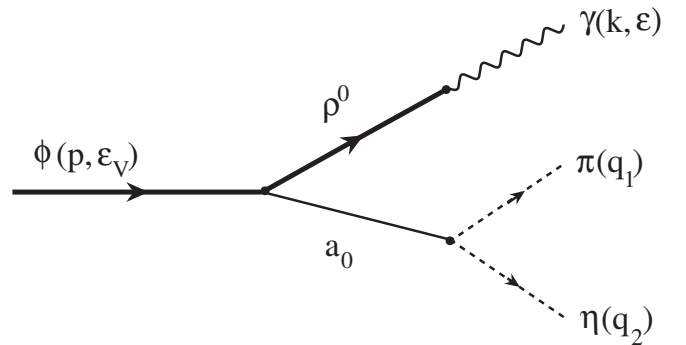


FIG. 1. Feynman diagram for  $\phi(p, \epsilon^V) \rightarrow \pi^0(q_1)\eta(q_2)\gamma(k, \epsilon)$  using an effective VVS term.

we use the simple  $a_0$  propagator:

$$D_{a_0}(q^2) = \frac{1}{m_{a_0}^2 - q^2 - im_{a_0}\Gamma_{a_0}}. \quad (2.7)$$

Also,  $q$  is the positive quantity:

$$q = [(p_0 - k_0)^2 - (\mathbf{p} - \mathbf{k})^2]^{1/2}. \quad (2.8)$$

Finally, the SPP-type coupling constant in Eq. (2.6) as well as others needed in this paper are defined from the

Lagrangian density:

$$\begin{aligned} \mathcal{L}_{\text{SPP}} = & -\gamma_{a_0\pi\eta} a_0^0 \partial_\mu \pi^0 \partial_\mu \eta - \frac{\gamma_{f_0\pi\pi}}{\sqrt{2}} f_0 \partial_\mu \pi^0 \partial_\mu \pi^0 \\ & - \frac{\gamma_{a_0 K \bar{K}}}{\sqrt{2}} a_0^0 \partial_\mu K^- \partial_\mu K^+ - \frac{\gamma_{f_0 K \bar{K}}}{\sqrt{2}} f_0 \partial_\mu K^- \partial_\mu K^+ \\ & + \dots \end{aligned} \quad (2.9)$$

The relations between these coefficients to  $A, B, C, D$  in Eq. (2.2) are given in Appendix C of Ref. [11]. The “ $q$  distribution”  $d\Gamma(\phi \rightarrow \pi^0 \eta \gamma)/dq$  is expressed as

$$\frac{d\Gamma(\phi \rightarrow \pi^0 \eta \gamma)}{dq} = \frac{\alpha}{768\pi^2} \left( \frac{M_\phi^2 - q^2}{M_\phi} \right)^3 \sqrt{\frac{[q^2 - (m_\eta + m_\pi)^2][q^2 - (m_\eta - m_\pi)^2]}{q^2}} (q^2 - m_\pi^2 - m_\eta^2)^2 |Y_{a_0}^{(\pi\eta)}|^2. \quad (2.10)$$

Discussion of the phase space integral is given, for example, in Ref. [20].

Now let us see how well we can fit the experimental data on the  $\pi^0 \eta$  invariant mass distribution in this model. We will use the inputs:  $m_{a_0} = 984.7$  MeV (from the PDG table [20]);  $\Gamma_{a_0} = 70$  MeV (from [21]);  $\gamma_{a_0\pi\eta} = -6.80$  GeV $^{-1}$  (from [21,22]).

Let us perform two types of fits for obtaining the best value of  $C_\phi^{a_0}$  (assuming  $\tilde{g}$  to be fixed at the value 4.04):

$$(I) \text{ use the data for all values of } q = m_{\pi^0 \eta}, \quad (2.11)$$

$$(II) \text{ use the data for } m_{\pi^0 \eta} \geq 850 \text{ MeV}. \quad (2.12)$$

The results are

$$\begin{aligned} (I) \quad C_\phi^{a_0} &= 3.7 \pm 0.1 \text{ GeV}^{-1}, & \chi^2/\text{d.o.f} &= 41/(32 - 1), \\ (II) \quad C_\phi^{a_0} &= 3.6 \pm 0.1 \text{ GeV}^{-1}, & \chi^2/\text{d.o.f} &= 32/(17 - 1). \end{aligned} \quad (2.13)$$

Figure 2 shows the resulting plots of  $dB(\phi \rightarrow \pi^0 \eta \gamma)/dq$  together with the experimental data. Note that, since only the combination  $\gamma_{a_0\pi\eta} C_\phi^{a_0}/\tilde{g}$  appears in our fitting procedure, the best fitted curve will not change even if we allow the values of  $\gamma_{a_0\pi\eta}$  and  $\tilde{g}$  to vary.

This model gives a poor fit to the experimental data in the energy region above 950 MeV. One possibility is that the fit may be improved by raising the mass of  $a_0$  above 984.7 MeV. Actually, Ref. [23] gives the best fit value as  $m_{a_0} = 995_{-10}^{+52}$  MeV. Let us then fit the  $a_0$  mass together with the value of  $C_\phi^{a_0}$ . The results are

$$\begin{aligned} (I) \quad C_\phi^{a_0} &= 4.0 \pm 0.1 \text{ GeV}^{-1}, & m_{a_0} &= 993.2 \pm 2.8 \text{ MeV}, \\ & \chi^2/\text{d.o.f} &= 39/(32 - 2), \\ (II) \quad C_\phi^{a_0} &= 3.9 \pm 0.1 \text{ GeV}^{-1}, & m_{a_0} &= 990.4 \pm 2.5 \text{ MeV}, \\ & \chi^2/\text{d.o.f} &= 31/(17 - 2). \end{aligned} \quad (2.14)$$

Note that the best fit value of  $m_{a_0}$  in case (II) is very close to the values shown in Ref. [23]. In Fig. 3, we plot  $dB(\phi \rightarrow \pi^0 \eta \gamma)/dq$  together with the experimental data. This figure shows that it is still difficult to reproduce the experimental data in the energy region above 950 MeV in the present model even if one allows the  $a_0$  mass to vary.

For comparison with the chiral symmetric case, we will now investigate the effect of using a nonderivative coupling at the  $a_0 \pi^0 \eta$  interaction vertex. This amounts to multiplying Eq. (2.10) by the factor:

$$\frac{(m_{a_0}^2 - m_\pi^2 - m_\eta^2)^2}{(q^2 - m_\pi^2 - m_\eta^2)^2}, \quad (2.15)$$

which has the effect of deemphasizing the high  $q$  region. It yields

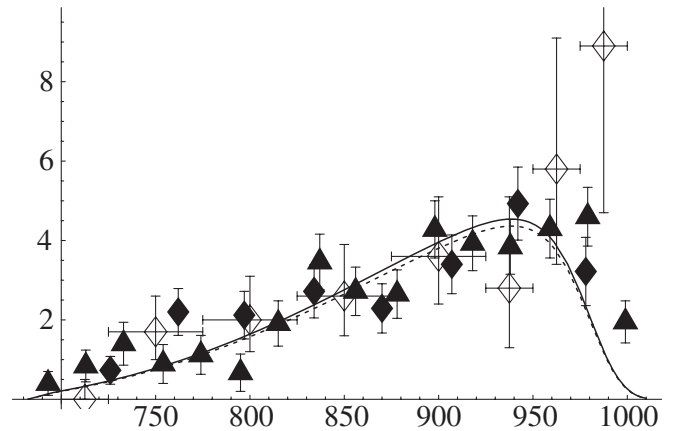


FIG. 2.  $dB(\phi \rightarrow \pi^0 \eta \gamma)/dq \times 10^7$  (in units of MeV $^{-1}$ ) as a function in the  $\pi^0 \eta$  invariant mass  $q = m_{\pi^0 \eta}$  (in MeV). The solid line shows the  $a_0$  contribution with the best fitted value  $C_\phi^{a_0} = 3.7$  GeV $^{-1}$ , and the dashed line shows that with  $C_\phi^{a_0} = 3.6$  GeV $^{-1}$ . Experimental data indicated by white diamonds are from the SND Collaboration in Ref. [23], and those by filled triangles and filled diamonds are shown in Ref. [41] extracted from the KLOE Collaboration in Ref. [42].

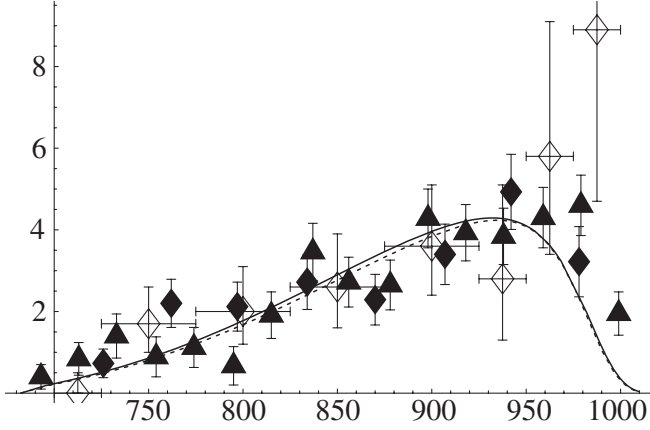


FIG. 3.  $dB(\phi \rightarrow \pi^0 \eta \gamma)/dq \times 10^7$  (in units of  $\text{MeV}^{-1}$ ) as a function in the  $\pi^0$ - $\eta$  invariant mass  $q = m_{\pi^0 \eta}$  (in MeV). The solid line shows the  $a_0$  contribution with the best fitted values  $C_\phi^{a_0} = 4.0 \text{ GeV}^{-1}$  and  $m_{a_0} = 993.2 \text{ MeV}$ , and the dashed line shows that with  $C_\phi^{a_0} = 3.9 \text{ GeV}^{-1}$  and  $m_{a_0} = 990.4 \text{ MeV}$ . Experimental data are as in Fig. 2.

$$\begin{aligned}
 \text{(I)} \quad C_\phi^{a_0} &= 2.13 \pm 0.07 \text{ GeV}^{-1}, \\
 \chi^2/\text{d.o.f} &= 113/(32 - 1), \\
 \text{(II)} \quad C_\phi^{a_0} &= 2.68 \pm 0.08 \text{ GeV}^{-1}, \\
 \chi^2/\text{d.o.f} &= 67.9/(17 - 1). \quad (2.16)
 \end{aligned}$$

Furthermore, Fig. 4 shows the plot of  $dB(\phi \rightarrow \pi^0 \eta \gamma)/dq$  together with the experimental data. Comparing this figure with Fig. 2 and the results in Eq. (2.16) with those in Eq. (2.13) indicates that the derivative coupling model gives a better fit. The nonderivative coupling factor clearly seems to wash out the resonance peak. It is also interesting to see the effect of allowing the  $a_0$  mass to vary along with  $C_\phi^{a_0}$  in a fit using the nonderivative coupling model. The results are

$$\begin{aligned}
 \text{(I)} \quad C_\phi^{a_0} &= 1.88 \pm 0.06 \text{ GeV}^{-1}, \\
 m_{a_0} &= 954.3 \pm 4.5 \text{ MeV}, \\
 \chi^2/\text{d.o.f} &= 93.6/(32 - 2), \\
 \text{(II)} \quad C_\phi^{a_0} &= 2.55 \pm 0.08 \text{ GeV}^{-1}, \\
 m_{a_0} &= 978.0 \pm 3.4 \text{ MeV}, \\
 \chi^2/\text{d.o.f} &= 66.6/(17 - 2). \quad (2.17)
 \end{aligned}$$

The plots are given in Fig. 5 and are seen to be in poorer agreement with the data than those in the derivative coupling case.

### B. $f_0(980)$ production

The treatment of the decay  $\phi \rightarrow \pi^0 \pi^0 \gamma$  assuming only the VVS-type interaction where S is identified as  $f_0(980)$  and subsequently decays to the two neutral pions proceeds

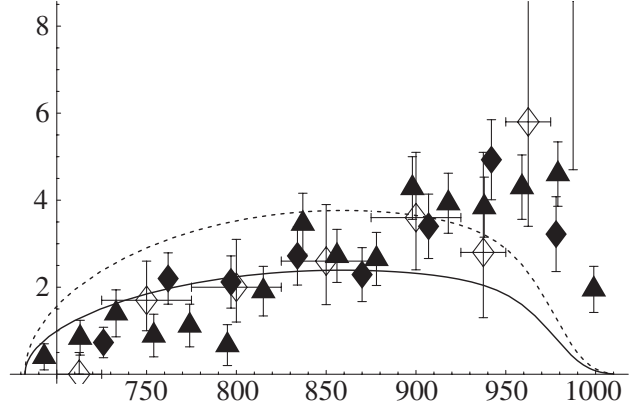


FIG. 4.  $dB(\phi \rightarrow \pi^0 \eta \gamma)/dq \times 10^7$  (in units of  $\text{MeV}^{-1}$ ) as a function in the  $\pi^0$ - $\eta$  invariant mass  $q = m_{\pi^0 \eta}$  (in MeV). The solid line shows the  $a_0$  contribution in the nonderivative coupling model with the best fit value  $C_\phi^{a_0} = 2.13 \text{ GeV}^{-1}$  and the dashed line shows that with  $C_\phi^{a_0} = 2.68 \text{ GeV}^{-1}$ . Experimental data are as in Fig. 2.

in a similar manner. Again it is found that the use of a chiral symmetric derivative-type interaction is to be preferred because it does not wash out the scalar resonance peak. However the overall fit to the  $\pi\pi$  invariant mass distribution is not good, again suggesting that the VVS-type of contribution is not the dominant one. In this case,  $d\Gamma(\phi \rightarrow \pi^0 \pi^0 \gamma)/dq$  is given by

$$\begin{aligned}
 \frac{d\Gamma(\phi \rightarrow \pi^0 \pi^0 \gamma)}{dq} &= \frac{\alpha}{1536\pi^2} \left( \frac{M_\phi^2 - q^2}{M_\phi} \right)^3 \\
 &\times \sqrt{q^2 - 4m_\pi^2} (q^2 - 2m_\pi^2)^2 |Y_{f_0}^{(\pi\pi)}|^2, \quad (2.18)
 \end{aligned}$$

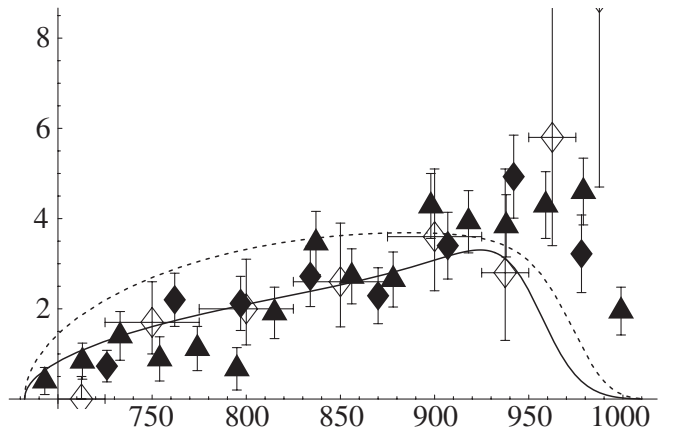


FIG. 5.  $dB(\phi \rightarrow \pi^0 \eta \gamma)/dq \times 10^7$  (in units of  $\text{MeV}^{-1}$ ) as a function in the  $\pi^0$ - $\eta$  invariant mass  $q = m_{\pi^0 \eta}$  (in MeV). The solid line shows the  $a_0$  contribution in the nonderivative coupling model with the best fit value  $C_\phi^{a_0} = 1.88 \text{ GeV}^{-1}$  and the dashed line shows that with  $C_\phi^{a_0} = 2.55 \text{ GeV}^{-1}$ . Experimental data are as in Fig. 2.

where

$$Y_{f_0}^{(\pi\pi)} = \frac{C_\phi^{f_0}}{\tilde{g}} D_{f_0}(q^2) \sqrt{2} \gamma_{f_0\pi\pi}. \quad (2.19)$$

The  $f_0$  propagator is

$$D_{f_0}(q^2) = \frac{1}{m_{f_0}^2 - q^2 - im_{f_0}\Gamma_{f_0}}, \quad (2.20)$$

and we will use the mass of the  $f_0(980)$  to be [24] 987 MeV. The coupling constant  $\gamma_{f_0\pi\pi}$  is related to the width of  $f_0$  as [24]

$$\Gamma_{f_0} = \frac{3}{64\pi} \frac{\gamma_{f_0\pi\pi}^2}{m_{f_0}} \sqrt{1 - \frac{4m_\pi^2}{m_{f_0}^2} (m_{f_0}^2 - 2m_\pi^2)^2}. \quad (2.21)$$

In Ref. [24] a treatment of  $\pi\pi$  scattering suggested  $\Gamma_{f_0} \approx 64.6$  MeV and correspondingly  $|\gamma_{f_0\pi\pi}| \approx 2.25$  GeV<sup>-1</sup>.

Considering both  $\pi\pi$  and  $\pi K$  scattering,  $\gamma_{f_0\pi\pi} \approx 1.47$  GeV<sup>-1</sup> and  $\Gamma_{f_0} \approx 27.6$  MeV were determined in Ref. [11].

Using for example  $|\gamma_{f_0\pi\pi}| = 1.47$  GeV<sup>-1</sup> let us next fit the value of  $C_\phi^{f_0}$  to the experimental data. Furthermore, to avoid any possible confusion with an expected low energy contribution from the  $\sigma$  we shall use experimental data only in the region

$$m_{\pi^0\pi^0} \geq 850 \text{ MeV}. \quad (2.22)$$

This yields

$$C_\phi^{f_0} \approx 9.3 \text{ GeV}^{-1}, \quad \chi^2/\text{d.o.f.} = 101/(17 - 1). \quad (2.23)$$

In Fig. 6, we show the resultant  $f_0$  contribution together with the experimental data [25,26].

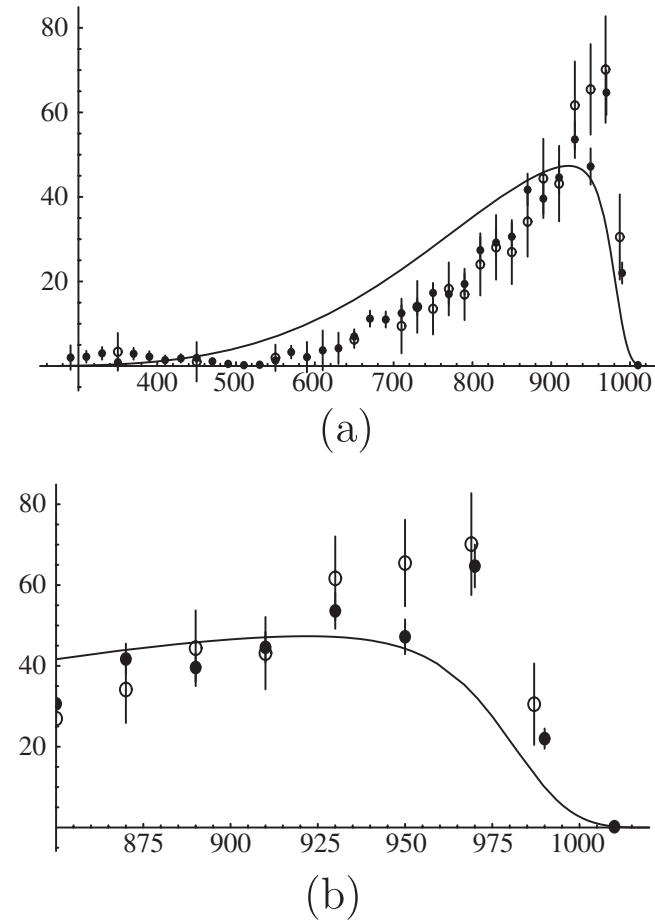


FIG. 6.  $dB(\phi \rightarrow \pi^0\pi^0\gamma)dq \times 10^8$  (in units of MeV<sup>-1</sup>) as a function of the dipion invariant mass  $q = m_{\pi^0\pi^0}$  (in MeV). The solid line shows the  $f_0$  contribution with  $C_\phi^{f_0} = 9.3$  GeV<sup>-1</sup>. (a) shows the result in the entire energy region, and (b) shows that in  $m_{\pi^0\pi^0} \geq 850$  MeV. Experimental data shown by open circles are from Ref. [25], and those by solid circles are from Ref. [26].

### III. CHARGED $K$ -LOOP CONTRIBUTION

Now let us explore the  $K$ -loop contributions to the radiative  $\phi$  decays. The relevant Feynman diagrams are shown in Fig. 7. Figures 7(c) and 7(d) each give the same result while Figs. 7(a) and 7(b) are required by gauge invariance. Notice from Eq. (2.3) that the direct photon-two pseudoscalar vertex vanishes in this model when  $k = 2$  is adopted, as we are doing here.<sup>3</sup> Thus the two pseudoscalars first couple to  $\rho$ ,  $\omega$  and  $\phi$  which then transform to a photon as shown in Figs. 7(c) and 7(d). The strong vector-two pseudoscalar interaction vertices may be read from the fourth term of Eq. (2.2) while the scalar-two pseudoscalar interaction vertices are derived from the  $A$ ,  $B$ ,  $C$  and  $D$  terms of this equation [and explicitly given in Eq. (2.9)].

Note again that the Lagrangian density of Eq. (2.2) treats all of the pseudoscalars, scalars and vectors in a consistent chiral invariant manner. It can be modified to include gauge invariant photon interactions by making the replacements:

$$\begin{aligned} v_\mu &\rightarrow \tilde{v}_\mu = v_\mu + \frac{1}{2}e\mathcal{A}_\mu(\xi Q\xi^\dagger + \xi^\dagger Q\xi), \\ p_\mu &\rightarrow \tilde{p}_\mu = p_\mu + \frac{1}{2}e\mathcal{A}_\mu(\xi Q\xi^\dagger - \xi^\dagger Q\xi), \\ \rho_\mu &\rightarrow \tilde{\rho}_\mu = \rho_\mu, \end{aligned} \quad (3.1)$$

where  $\mathcal{A}$  and  $Q$  were defined after Eq. (2.3). Under an infinitesimal electromagnetic gauge transformation with  $\delta\mathcal{A}_\mu = \partial_\mu\lambda(x)$ ,  $\tilde{p}_\mu$  and  $\tilde{v}_\mu - \tilde{g}\tilde{\rho}_\mu$  in Eq. (3.1) do not contain any terms proportional to  $\partial_\mu\lambda(x)$ . When substituted into Eq. (2.2), the above replacements yield, in addition to Eq. (2.3) the four field photon interaction terms in the Lagrangian density:

<sup>3</sup>In the present analysis, we just use  $k = 2$  for simplicity in calculation so that two kaons couple to gamma only through vector meson intermediate lines keeping vector meson dominance.

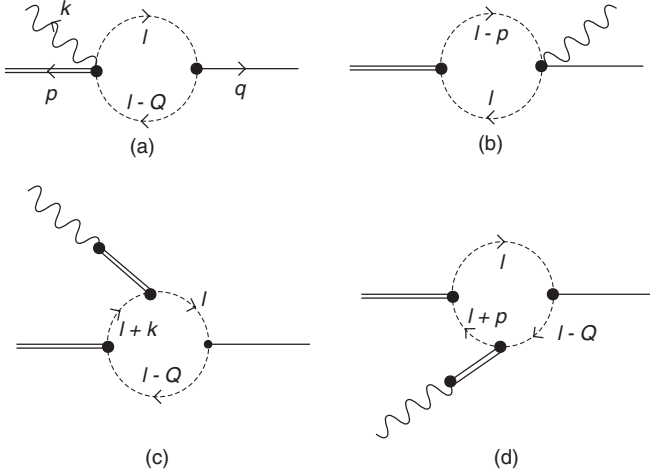


FIG. 7. Feynman diagrams for the charged  $K$ -loop contributions to  $\phi(p, \epsilon^V) \rightarrow a_0(Q) + \gamma(k, \epsilon)$ . The solid lines denote the  $a_0$  meson, the wavy lines the photon, the double solid lines the vector mesons ( $\rho, \omega, \phi$ ) and the dashed lines the  $K$  meson.  $p, k$  and  $Q$  are the momenta of the  $\phi$  meson, the photon and the  $a_0(980)$ , respectively, and  $l$  is the loop momentum.

$$\frac{em_v^2}{\tilde{g}F_\pi^2} \mathcal{A}_\mu \phi_\mu K^+ K^- + i \frac{e\gamma_{aKK}}{\sqrt{2}} \times \mathcal{A}_\mu a_0^0 (K^+ \partial_\mu K^- - K^- \partial_\mu K^+) + \dots, \quad (3.2)$$

where  $\phi_\mu$  is the  $\phi$ -meson field and  $a_0^0$  is the neutral  $a_0(980)$  scalar meson field.<sup>4</sup> Now it is straightforward to obtain the  $K$ -loop amplitudes (with the assumption  $k = 2$ ) for  $\phi(p, \epsilon^V) \rightarrow a_0(Q) + \gamma(k, \epsilon)$ :

$$\begin{aligned} S_a &= h \int \frac{d^4 l}{i(2\pi)^4} \frac{[l \cdot (Q - l)][\epsilon \cdot \epsilon^V]}{[l^2 + m_K^2][(Q - l)^2 + m_K^2]}, \\ S_b &= -\frac{h}{2} \int \frac{d^4 l}{i(2\pi)^4} \frac{[(2l - p) \cdot \epsilon^V][(2l - p) \cdot \epsilon]}{[l^2 + m_K^2][(p - l)^2 + m_K^2]}, \\ S_c &= S_d \\ &= -\frac{h}{2} \int \frac{d^4 l}{i(2\pi)^4} \\ &\quad \times \frac{[l \cdot (Q - l)][(2l + k) \cdot \epsilon][(2l + k - Q) \cdot \epsilon^V]}{[l^2 + m_K^2][(Q - l)^2 + m_K^2][(k + l)^2 + m_K^2]}, \end{aligned} \quad (3.3)$$

where

<sup>4</sup>The terms such as  $\epsilon^{abc} \epsilon_{def} N_a^d (\tilde{g}\rho_\mu - v_\mu)_b^c (\tilde{g}\rho_\mu - v_\mu)_c^f$  can be added into the Lagrangian (2.2). Although they do not contribute at tree level to the radiative decays studied in the present analysis, they generate the vertex of type  $SV\gamma PP$ , which gives the quantum correction to  $SV\gamma$  vertex. Since this quantum correction does not depend on the external momenta, its contribution is absorbed into the redefinition of the effective  $SV\gamma$  coupling  $C_\gamma^S$ .

$$h = \frac{em_v^2 \gamma_{aKK}}{\sqrt{2} \tilde{g} F_\pi^2} \approx \sqrt{2} e \tilde{g} \gamma_{aKK}, \quad (3.4)$$

and the KSRF relation was used in the last step. Note the quantity defined in Eq. (2.8),  $q^2 = -Q^2$ . To get the amplitude for the decay  $\phi \rightarrow f_0 \gamma$  we should replace  $\gamma_{aKK}$  by  $\gamma_{fKK}$  in Eq. (3.4).

The next step is to regulate the divergences which occur in these amplitudes. We employ the dimensional regularization scheme and thus continue from 4 to  $d$  space-time dimensions according to the formula:

$$\int \frac{d^d l}{i(2\pi)^d} \frac{1}{(l^2 + s)^n} = \frac{\Gamma(n - d/2)}{(4\pi)^{d/2} \Gamma(n) s^{n-d/2}}, \quad (3.5)$$

where  $n$  is an integer while  $s$  is arbitrary. The physical amplitudes will emerge in the limit when  $\epsilon = 4 - d \rightarrow 0$ . It is convenient to define

$$\frac{1}{\bar{\epsilon}} = \frac{2}{\epsilon} - \gamma + \ln(4\pi), \quad (3.6)$$

where  $\gamma \approx 0.577$  is the Euler-Mascheroni constant.

For  $S_a$  we use the identity  $l \cdot Q - l^2 = -1/2[(l - Q)^2 + m_K^2] - 1/2(l^2 + m_K^2) + (m_K^2 + Q^2/2)$  to write

$$S_a = ih \delta_{\mu\nu} \epsilon_\nu^V(p) \epsilon_\nu(k) [-A_0(m_K^2) + \frac{1}{2}(2m_K^2 + Q^2)B_0(Q^2)], \quad (3.7)$$

where [27]

$$A_0(m_K^2) = \int \frac{d^d l}{i(2\pi)^d} \frac{1}{l^2 + m_K^2}, \quad (3.8)$$

$$B_0(Q^2) = \int \frac{d^d l}{i(2\pi)^d} \frac{1}{[l^2 + m_K^2][(l - Q)^2 + m_K^2]}.$$

For  $S_b$  we define

$$S_b = -i \frac{h}{2} \epsilon_\mu^V(p) \epsilon_\nu(k) B_{\mu\nu}(p), \quad (3.9)$$

$$B_{\mu\nu}(p) = \int \frac{d^d l}{i(2\pi)^d} \frac{(2l - p)_\mu (2l - p)_\nu}{[l^2 + m_K^2][(p - l)^2 + m_K^2]}.$$

Finally, for the triangle diagrams we similarly rearrange the numerator to get

$$\begin{aligned} S_c &= S_d \\ &= -i \frac{h}{2} \epsilon_\mu^V(p) \epsilon_\nu(k) \left[ -\frac{1}{2} B_{\mu\nu}(k) + Q_\mu B_\nu(-k) \right. \\ &\quad \left. + \frac{1}{2} Q_\mu k_\nu B_0(k^2) - \frac{1}{2} B_{\mu\nu}(p) - B_\mu(p) Q_\nu \right. \\ &\quad \left. + \frac{1}{2} p_\mu Q_\nu B_0(p^2) + \frac{1}{2} (2m_K^2 + Q^2) X_{\mu\nu}(p, k) \right], \end{aligned} \quad (3.10)$$

wherein  $B_0(p^2)$  and  $B_{\mu\nu}(p)$  have been already defined while

$$B_\mu(p) = \int \frac{d^d l}{i(2\pi)^d} \frac{l_\mu}{[l^2 + m_K^2][(l-p)^2 + m_K^2]}, \quad (3.11)$$

and

$$X_{\mu\nu}(p, k) = \int \frac{d^d l}{i(2\pi)^d} \times \frac{(2l+k-Q)_\mu(2l+k)_\nu}{[l^2 + m_K^2][(Q-l)^2 + m_K^2][(k+l)^2 + m_K^2]}. \quad (3.12)$$

Note that  $k^2 = 0$  since it corresponds to a physical photon momentum.

Using Feynman's trick for combining denominators and Eqs. (3.5) and (3.6) we evaluate the integral  $B_0(p^2)$  near  $d = 4$ :

$$B_0(p^2) = \frac{1}{(4\pi)^2} \left[ \frac{1}{\bar{\epsilon}} - F_0(p^2) \right], \quad (3.13)$$

$$F_0(p^2) = \int_0^1 dx \ln[m_K^2 - x(x-1)p^2].$$

We also find

$$B_\mu(p) = \frac{1}{2} p_\mu B_0(p^2). \quad (3.14)$$

The presence of a pole at  $d = 4$  indicated by the term  $1/\bar{\epsilon}$  corresponds, of course, to a logarithmic divergence in the cutoff regularization method.

Using the integrals defined above we can compactly write the total amplitude as

$$S = S_a + S_b + S_c + S_d$$

$$= i \frac{\hbar}{2} \epsilon_\mu^V(p) \epsilon_\nu(k) [\delta_{\mu\nu} (-2A_0(m_K^2) + (2m_K^2 + Q^2)B_0(Q^2)) + B_{\mu\nu}(k) - (2m_K^2 + Q^2)X_{\mu\nu}(p, k)]. \quad (3.15)$$

Notice, in particular, that the contribution of  $S_b$  has canceled out against a piece of the triangle diagrams.

The evaluation of an integral of the form  $B_{\mu\nu}(p)$  is a little more complicated. We use covariance (in  $d$  dimensions) to relate it to the other integrals as

$$B_{\mu\nu}(p) = \delta_{\mu\nu} \frac{4}{1-d} \left[ -\frac{A_0(m_K^2)}{2} + \left( m_K^2 + \frac{p^2}{4} \right) B_0(p^2) \right]$$

$$+ p_\mu p_\nu \left[ \frac{4}{p^2} \left( \left( 1 + \frac{1}{2} \frac{d}{1-d} \right) A_0(m_K^2) - m_K^2 \left( 1 + \frac{d}{1-d} \right) B_0(p^2) - \frac{p^2}{4} \frac{d}{1-d} B_0(p^2) \right) - B_0(p^2) \right]. \quad (3.16)$$

We see that  $B_{\mu\nu}$  contains the integral  $A_0(m_K^2)$  which is noted from Eq. (3.8) to involve a quadratic divergence in the cutoff regularization scheme. In the dimensional regu-

larization approach this corresponds [28] to a pole at  $d = 2$ , as may be seen from Eq. (3.5). It is necessary to check that this divergence cancels out in the total amplitude. This may be done by using Eq. (3.16) to get, near  $d = 2$ ,

$$B_{\mu\nu}(k)|_{k^2=0} = 2A_0(m_K^2) \delta_{\mu\nu} + \dots, \quad (3.17)$$

where the three dots indicate terms not containing  $A_0(m_K^2)$ . Substituting this into Eq. (3.15) (considered at  $d = 2$ ) shows that all dependence on  $A_0(m_K^2)$  at  $d = 2$  is canceled, as desired. We interpret this as the cancellation of the quadratic divergences in the individual diagrams.

For the physical case we must consider, of course, the amplitude evaluated near  $d = 4$ . The integral  $A_0(m_K^2)$  is, near  $d = 4$ ,

$$A_0(m_K^2) = -\frac{m_K^2}{(4\pi)^2} \left[ \frac{1}{\bar{\epsilon}} + 1 - \ln(m_K^2) \right]. \quad (3.18)$$

Using Eq. (3.16) we find for  $B_{\mu\nu}(k)$  near  $d = 4$  and  $k^2 = 0$ :

$$B_{\mu\nu}(k) = 2A_0(m_K^2) \delta_{\mu\nu} + \frac{1}{3(4\pi)^2} k_\mu k_\nu \left[ \frac{1}{\bar{\epsilon}} - \ln(m_K^2) + \frac{2}{3} \right], \quad (3.19)$$

wherein the first term was separated for convenience. Note that the  $k_\mu k_\nu$  term will not contribute to the physical amplitude because it gets multiplied by the photon polarization vector  $\epsilon_\nu(k)$ . Now substituting Eq. (3.19) into the total amplitude, Eq. (3.15), shows that its effect is simply to cancel the  $-2A_0(m_K^2)$  term.

To evaluate the remaining  $X_{\mu\nu}(p, k)$  term we first use covariance to express it as

$$X_{\mu\nu}(p, k) = \delta_{\mu\nu} X_1 + p_\mu p_\nu X_2 + k_\mu k_\nu X_3 + p_\mu k_\nu X_4 + k_\mu p_\nu X_5, \quad (3.20)$$

where each of the  $X_i$  depends on  $p^2$  and  $p \cdot k$ . The  $X_i$  may be determined by calculating  $X_{\mu\mu}$ ,  $k_\mu X_{\mu\nu}$ ,  $p_\nu X_{\mu\nu}$  and  $k_\mu p_\nu X_{\mu\nu}$  both from Eq. (3.20) and from Eq. (3.12). This leads to the relations (remembering  $k^2 = 0$ )

$$X_2 = 0,$$

$$B_0(Q^2) = X_1 + k \cdot p X_5,$$

$$0 = k \cdot p X_3 + p^2 X_4,$$

$$X_5 = \frac{1}{(p \cdot k)^2} \left[ \frac{p^2}{d-2} (B_0(Q^2) - B_0(p^2)) + \left( p \cdot k + \frac{Q^2 - p^2}{d-2} \right) B_0(Q^2) + \frac{4m_K^2 k \cdot p}{d-2} C(p^2, k \cdot p) \right], \quad (3.21)$$

where the finite integral  $C(p^2, k \cdot p)$  is given by



$$C(p^2, k \cdot p) = \int \frac{d^4 l}{i(2\pi)^4} \times \frac{1}{[l^2 + m_K^2][(l-Q)^2 + m_K^2][(l+k)^2 + m_K^2]}. \quad (3.22)$$

Actually, only the coefficients  $X_1$  and  $X_5$  remain after  $X_{\mu\nu}$  is multiplied by the polarization vectors of the photon and  $\phi$  meson; furthermore these two coefficients are related as above. Substituting back into the total amplitude, Eq. (3.15) and making use of the cancellation between the  $A_0(m_K^2)$  and  $B_{\mu\nu}(k)$  terms discussed before, yields

$$S = i \frac{h}{2} \epsilon_\mu^V(p) \epsilon_\nu(k) \left( -\frac{\delta_{\mu\nu}}{p \cdot k} + \frac{k_\mu p_\nu}{(p \cdot k)^2} \right) (2m_K^2 + Q^2) \times \left[ \frac{p^2}{2} \{B_0(Q^2) - B_0(p^2)\} + 2m_K^2 (p \cdot k) C(p^2, p \cdot k) - \frac{p \cdot k}{(4\pi)^2} \right]. \quad (3.23)$$

Note that the last term arises from the  $1/\epsilon$  term in  $B_0(Q^2)$  multiplying the leading  $\epsilon$  term of its factor. From Eq. (3.13) we see that the logarithmic divergences cancel out of the difference ( $B_0(Q^2) - B_0(p^2)$ ). Thus the final amplitude is completely finite; both the logarithmic and quadratic divergences have been seen to cancel using regularized expressions for everything. The quadratic divergences arose in the first place because of the derivative-type interactions required by use of the nonlinear sigma model terms to describe the pseudoscalar meson interactions. In addition, the starting Lagrangian treated the vector and scalar mesons in the same chiral invariant framework.

Evaluation of the finite integrals in Eq. (3.23) yields the final expression for the Feynman amplitude,  $iS$ ,

$$iS = -\frac{h}{2} \frac{1}{(4\pi)^2} \epsilon_\mu^V(p) \epsilon_\nu(k) \left( -\frac{\delta_{\mu\nu}}{p \cdot k} + \frac{k_\mu p_\nu}{(p \cdot k)^2} \right) \times (2m_K^2 + Q^2) \left\{ -p \cdot k + \frac{p^2}{2} \left( \sigma(p^2) \left[ \ln \frac{1 + \sigma(p^2)}{1 - \sigma(p^2)} - i\pi \right] - \sigma(Q^2) \left[ \ln \frac{1 + \sigma(Q^2)}{1 - \sigma(Q^2)} - i\pi \right] \right) + \frac{m_K^2}{2} \left( \left[ \ln \frac{1 + \sigma(p^2)}{1 - \sigma(p^2)} - i\pi \right]^2 - \left[ \ln \frac{1 + \sigma(Q^2)}{1 - \sigma(Q^2)} - i\pi \right]^2 \right) \right\}, \quad (3.24)$$

where

$$\sigma(p^2) = \sqrt{1 + \frac{4m_K^2}{p^2}}, \quad \sigma(Q^2) = \sqrt{1 + \frac{4m_K^2}{Q^2}}. \quad (3.25)$$

Note that Eq. (3.24) holds only in the kinematical range where  $-Q^2 = q^2 > 4m_K^2$ ; the positive quantity,  $q$  was also defined in Eq. (2.8). Furthermore note that  $p^2 = -m_\phi^2$ . In

the kinematical range where  $-Q^2 = q^2 < 4m_K^2$ , one should replace

$$\left[ \ln \frac{1 + \sigma(Q^2)}{1 - \sigma(Q^2)} - i\pi \right] \rightarrow -2i \tan^{-1} \frac{1}{\tilde{\sigma}(Q^2)}, \quad (3.26)$$

$$\sigma(Q^2) \rightarrow i\tilde{\sigma}(Q^2) = i\sqrt{-1 - \frac{4m_K^2}{Q^2}},$$

in Eq. (3.24) above.

#### IV. COMPARING THE $K$ LOOP WITH EXPERIMENT

The expression in Eq. (3.24) describes the decay  $\phi \rightarrow a_0 \gamma$ . To get the Feynman amplitude for  $\phi \rightarrow \pi^0 \eta \gamma$ , we should multiply Eq. (3.24) by the factor  $(q_1 \cdot q_2) D_{a_0}(q^2) \gamma_{a_0 \pi \eta}$ , where  $D_{a_0}(q^2)$  was defined in Eq. (2.7). This assumes a simple form for the  $a_0$  propagator, which can only be an approximation. However our main concern here is an initial exploration of the resonance region in the present framework so it seems reasonable for now. We write the resulting Feynman amplitude as

$$iS(\phi \rightarrow \pi^0 \eta \gamma) = e(q_1 \cdot q_2) X_{a_0}^{(\pi\eta)} [(p \cdot k)(\epsilon^V \cdot \epsilon) - (p \cdot \epsilon)(k \cdot \epsilon^V)], \quad (4.1)$$

which thereby defines  $X_{a_0}^{(\pi\eta)}$ . Note that the sum  $X_{a_0}^{(\pi\eta)} + Y_{a_0}^{(\pi\eta)}$ , where  $Y_{a_0}^{(\pi\eta)}$  is defined in Eq. (2.6), would correspond to a model containing both the  $K$ -loop contribution to the resonant amplitude as well as a point vertex contribution to the resonant amplitude. For now we focus on the  $K$ -loop contribution. The decay spectrum shape,  $d\Gamma/dq$  is then obtained by replacing  $Y_{a_0}^{(\pi\eta)}$  in Eq. (2.10) by  $X_{a_0}^{(\pi\eta)}$ . Conventionally, one uses instead,

$$\frac{dB(\phi \rightarrow \pi^0 \eta \gamma)}{dq} = \frac{1}{\Gamma(\phi)} \frac{d\Gamma(\phi \rightarrow \pi^0 \eta \gamma)}{dq}, \quad (4.2)$$

where  $\Gamma(\phi) = 4.26$  MeV.

In Sec. II A we observed that, even though the use of the derivative-type SPP coupling helped somewhat, the tree interaction involving the  $a_0(980)$  resonance was unable to explain the shape of the peak at large  $q$  in the experimental data for  $dB(\phi \rightarrow \pi^0 \eta \gamma)/dq$ . Now we will look at the result of using the  $K$ -loop amplitude for this purpose. Taking [20]  $m_a = 985$  MeV and  $\Gamma_a = 50$ – $100$  MeV, the only quantity which is not well known is the product of the scalar meson coupling constants  $\gamma_{aKK} \gamma_{a\pi\eta}$ . In Fig. 8, it is shown that a choice  $\gamma_{aKK} \gamma_{a\pi\eta} = 125$  GeV<sup>-2</sup> can nicely explain the shape of the experimental data in the region of  $q$  near the  $a_0(980)$  resonance.

For  $q$  below the resonance region, the  $K$ -loop contribution in the present model falls off rapidly, as one might reasonably expect with a derivative coupling, and lies lower than the data points. In addition to the nonresonant background [3] which is usually included to explain this

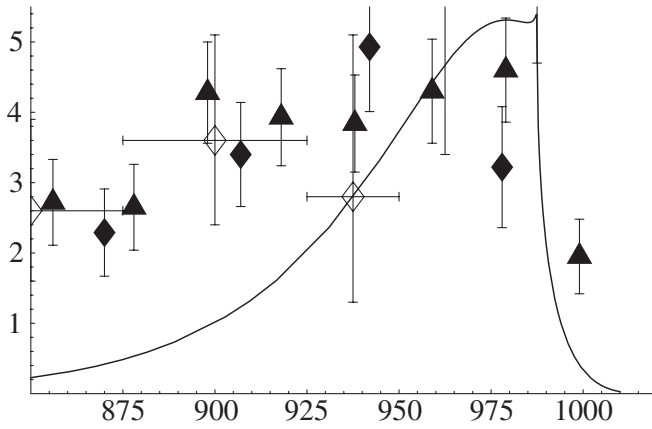


FIG. 8. Predicted  $dB(\phi \rightarrow \pi^0 \eta \gamma)/dq$  in the region of the  $a_0(980)$  resonance with  $\gamma_{aKK} \gamma_{a\pi\eta} = 125 \text{ GeV}^{-2}$  and  $\Gamma_a = 0.1 \text{ GeV}$ . The vertical scale has units  $10^{-7} \text{ MeV}^{-1}$ . Experimental data are as in Fig. 2.

region, there might be some tree level resonance production which was observed in Fig. 2 to peak around 950 MeV.

The main feature of the data is that there is a very rapid falloff with apparent discontinuity of the slope, when  $q$  reaches the  $K\bar{K}$  threshold. This is a clear signal for the importance of the  $K$ -loop contribution. One may see this feature by referring to Fig. 9, for which the  $a_0(980)$  mass has been artificially lowered to 970 MeV. Comparing with the previous figure shows that the sharp falloff is exactly the same in both cases, clearly unaffected by the difference of assumed resonance masses in the two cases. The difference in masses, on the other hand, shows up as a difference in position of the peaks. It should be remarked that the peak position is also affected by the decreasing phase space with increasing  $q$ . This characteristic feature of the  $K$ -loop contribution was first illustrated by Achasov [29] by considering the behavior of the result with lowered values of the  $K$ -meson mass.

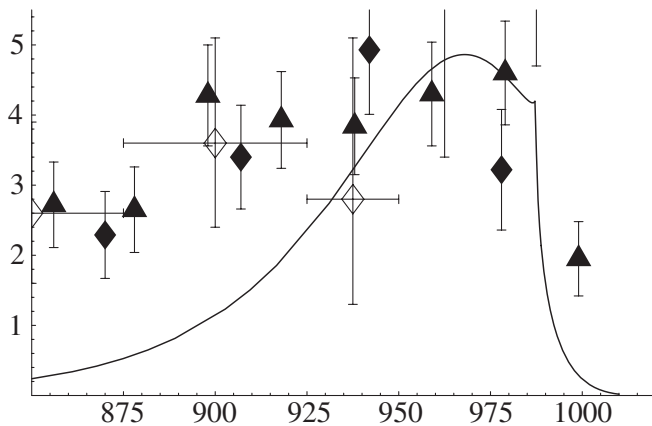


FIG. 9. Predicted  $dB(\phi \rightarrow \pi^0 \eta \gamma)/dq$  in the region of the  $a_0(980)$  resonance but where the  $a_0$  mass was artificially lowered to 970 MeV. Here  $\gamma_{aKK} \gamma_{a\pi\eta} = 115 \text{ GeV}^{-2}$  and  $\Gamma_a = 0.1 \text{ GeV}$ . Experimental data are as in Fig. 2.

Next, let us check the dependence of the prediction on the width of  $a_0(980)$ . Figure 10 shows that the predicted  $dB(\phi \rightarrow \pi^0 \eta \gamma)/dq$  in the region of the  $a_0(980)$  resonance with  $\gamma_{aKK} \gamma_{a\pi\eta} = 95 \text{ GeV}^{-2}$  and  $\Gamma_a = 0.05 \text{ GeV}$ . Comparing this prediction with that given in Fig. 8, we see that the smaller  $a_0$  width gives a sharper peak, and that a smaller value of  $\gamma_{aKK} \gamma_{a\pi\eta}$  can also reproduce the experimental data at the peak position. For further decreasing the value of  $\gamma_{aKK} \gamma_{a\pi\eta}$  the inclusion of the  $K$ -loop correction into the propagator of  $a_0(980)$  may be important as pointed out in Ref. [29].

The  $K$ -loop contribution to the branching distribution,  $dB(\phi \rightarrow \pi^0 \pi^0 \gamma)/dq$ , may be similarly evaluated and compared to experiment. There is similarly a problem for the tree level resonance model to reproduce this experimental shape in the high  $q$  region. The  $K$ -loop amplitude  $\phi \rightarrow f_0(980) \gamma$  is given by Eq. (3.24) wherein the overall factor  $h$  is now obtained by replacing  $\gamma_{aKK}$  in Eq. (3.4) by  $\gamma_{fKK}$ . To get the Feynman amplitude for  $\phi \rightarrow \pi^0 \pi^0 \gamma$ , we should multiply Eq. (3.24) by the factor  $\sqrt{2}(q_1 \cdot q_2) D_{f_0}(q^2) \gamma_{f_0 \pi \pi}$ , where  $D_{f_0}(q^2)$  was defined in Eq. (2.20). This defines  $X_{f_0}^{(\pi\pi)}$  as in Eq. (4.1). The spectrum shape is determined by using Eq. (2.18) with  $X_{f_0}^{(\pi\pi)}$  replacing  $Y_{f_0}^{(\pi\pi)}$ .

Taking [20]  $m_f = 980 \pm 10 \text{ MeV}$  and  $\Gamma_f = 40\text{--}100 \text{ MeV}$ , the only quantity which is not well known is the product of the scalar meson coupling constants  $\gamma_{fKK} \gamma_{f\pi\pi}$ . In Fig. 11, it is shown that a choice  $\gamma_{aKK} \gamma_{f\pi\pi} = 86 \text{ GeV}^{-2}$  can nicely explain the shape of the experimental data in the region of  $q$  near the  $f_0(980)$  resonance.

As in the case of the  $\phi \rightarrow \pi^0 \eta \gamma$  process, the  $K$ -loop description of  $dB/dq$  only explains the upper  $q$  region near the scalar resonance. To cover the lower  $q$  region some nonresonant background [3] is required. Possibly a tree

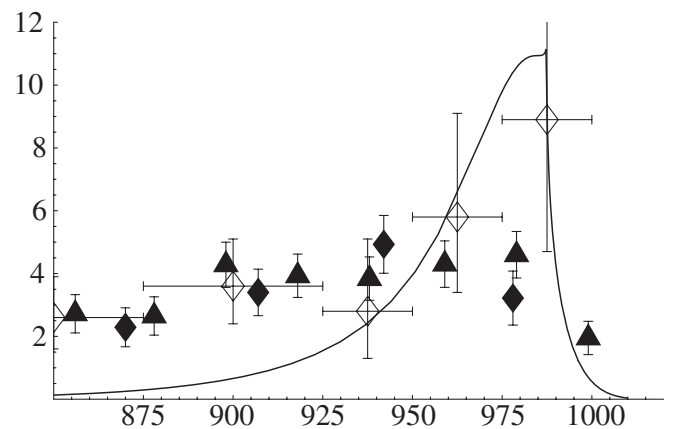


FIG. 10. Predicted  $dB(\phi \rightarrow \pi^0 \eta \gamma)/dq$  in the region of the  $a_0(980)$  resonance with  $\gamma_{aKK} \gamma_{a\pi\eta} = 95 \text{ GeV}^{-2}$  and  $\Gamma_a = 0.05 \text{ GeV}$ . Experimental data are as in Fig. 2.

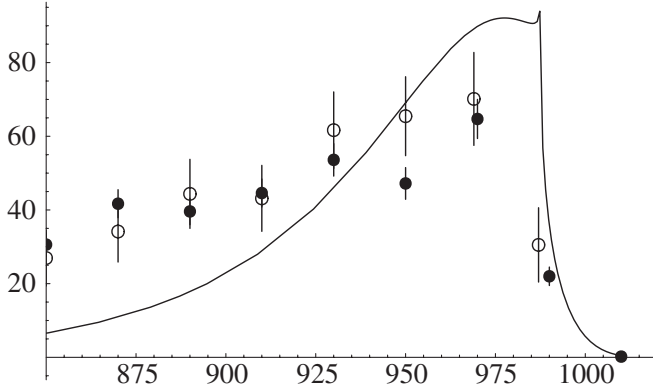


FIG. 11. Predicted  $dB(\phi \rightarrow \pi^0 \pi^0 \gamma)/dq$  in the region of the  $f_0(980)$  resonance with  $\gamma_{fKK} \gamma_{f\pi\pi} = 86 \text{ GeV}^{-2}$  and  $\Gamma_f = 0.1 \text{ GeV}$ . The vertical scale has units  $10^{-8} \text{ MeV}^{-1}$ .

level resonant background, corresponding to using  $X_{f_0}^{(\pi\pi)} + Y_{f_0}^{(\pi\pi)}$  in Eq. (2.18), would also be appropriate.

In both cases considered in this section, it is also desirable to include the effects of using multichannel scalar meson propagators [30] for a better approximation to the detailed dynamics. A very recent treatment of the  $\phi \rightarrow \pi^0 \pi^0 \gamma$  process in this framework is given in [31].

## V. SUMMARY AND DISCUSSION

Historically, the study of elementary particle spectroscopy has been built around the organization of these particles into SU(3) flavor multiplets and the consequent predicted (broken symmetry) mass formulas and interaction vertices. The still mysterious scalars can be expected to yield up some of their secrets by this type of analysis. Indeed some recent analyses have already been carried out [11,32–35]. The most dramatic feature is that the light scalars appear to exhibit, as originally suggested by Jaffe [36], a reverse mass ordering compared to the other meson multiplets.

In Ref. [6] an attempt was made to extend the SU(3) analysis to relate all the decays of the types  $S \rightarrow \gamma\gamma$ ,  $V \rightarrow S\gamma$  and  $S \rightarrow V\gamma$  to each other by using a simple effective VVS pointlike interaction, together with vector meson dominance. The analogous assumption [7] of a pointlike VVP structure was very successful [37] in phenomenologically correlating  $P \rightarrow \gamma\gamma$ ,  $V \rightarrow P\gamma$  and  $P \rightarrow V\gamma$  decays. Such an approach was the original motivation which led to the present investigation. In Sec. II we compared the spectrum shape of the decays  $\phi \rightarrow \eta \pi^0 \gamma$ , measuring the effects of an intermediate  $a_0(980)$  resonance and  $\phi \rightarrow \pi^0 \pi^0 \gamma$ , measuring the effects of an intermediate  $f_0(980)$  resonance, in the pointlike VVS model with the corresponding experimental observations. It was found that the resonant peaks in the model were pushed lower due to decreasing phase space. This contrasted with experiment which does not indicate this effect. On the other hand, if

one were to use a tree model of this type with nonderivative SPP-type couplings, the resonant peaks were seen to get completely washed out. This would appear to be an advantage for the derivative coupling, which is dictated by chiral symmetry in the present framework. Nevertheless, since even with derivative coupling the spectrum shape is not very well fitted, there must be another mechanism at work.

Now, it has been emphasized [29] that the  $K$ -loop model for the  $\phi$  radiative decays constitutes a special mechanism which does give a characteristic spectrum shape in agreement with experiment. This is readily understandable since the  $\phi(1020)$  meson is just a little bit heavier than the two  $K$  mesons which comprise its main decay product. We thus studied the  $K$ -loop diagrams using the chiral Lagrangian of pseudoscalars, vectors and scalars given in Eqs. (2.2) and (2.4) with the relevant photon terms introduced by the substitutions shown in Eq. (3.1). Most of the calculations of this process have not started from a chiral symmetric Lagrangian and have thus used nonderivative-type SPP-type interaction vertices. The use of a derivative coupling introduces an extra complication in that there is a new diagram, shown as Fig. 7(b). In addition, individual diagrams now contain quadratic as well as logarithmic divergences. It is known that these divergences are forced to cancel from gauge invariance. However we have used the dimensional regularization scheme and shown explicitly in Sec. III that both the log and quadratic divergences cancel in the regularized expressions. This may be of some interest in dealing with processes of the present type.

In Sec. IV, we observed that the shape of the  $a_0(980)$  and  $f_0(980)$  resonance regions in the  $\phi$  radiative decays could be explained by the corresponding  $K$ -loop amplitudes. Furthermore, it was evident that the characteristic sharp drop in the amplitude at large  $q^2$  was associated with the  $K\bar{K}$  threshold rather than with the falloff of the resonance away from its peak. For this work, we used the coupling constant products  $\gamma_{aKK} \gamma_{a\pi\eta}$  and  $\gamma_{fKK} \gamma_{f\pi\pi}$  respectively as fitting parameters for the  $\phi$  radiative decay spectra into  $\pi^0 \eta$  and  $\pi^0 \pi^0$ . Elsewhere, we plan to study more precisely the values of these coupling constants obtained by comparing with experiment, chiral models of meson-meson scattering in which the same interactions are used. We also will study how the pointlike diagrams with resonant contributions discussed in Sec. II can be used in conjunction with the  $K$ -loop diagrams to improve the fit to the resonant region. This will presumably become even more interesting when more data points become available. Another point of interest concerns the extent to which the various SPP coupling constants can be correlated assuming a single nonet of scalars. This arises because there is some evidence [38] that two scalar nonets (one presumably made from four quarks and the other from two quarks) mix to make up the physical scalar states. A recent exploration of the effect of such a mixture on  $\phi(1020)$  radiative decays has been given in Ref. [39]. Still another correction to the simple

picture employed here would be to use more realistic resonance propagators by including pseudoscalar loops [30].

Of course, in order to make a careful comparison with experiment one should include nonresonant contributions which are expected to dominate for small  $q$ . These will include the emission of a pion with a virtual  $\rho$  which subsequently decays into  $\pi\gamma$  (and similar diagrams leading to a  $\pi^0\eta\gamma$  final state) as discussed in Ref. [3]. There will also be nonresonant contributions from the  $K$ -loop diagrams. A variety of interference mechanisms to explain the full spectrum are discussed in Ref. [40]. It should be noted that the “background” contributions may very well have a nontrivial effect also in the resonance region itself.

Using the results obtained here and taking into account the features just discussed, we will continue to study the  $\phi$

radiative decays with the expectation that it may contribute to the understanding of the puzzling scalar mesons and ultimately to low energy QCD.

## ACKNOWLEDGMENTS

We would like to thank A. Abdel-Rehim, N. N. Achasov, A. H. Fariborz, and F. Sannino for very helpful discussions. The work of D. B. is supported by the Royal Society. The work of M. H. is supported in part by the Daiko Foundation No. 9099, the 21st Century COE Program of Nagoya University provided by the Japan Society for the Promotion of Science (15COEG01), and the JSPS Grant-in-Aid for Scientific Research (c) (2) No. 16540241. The work of J. S. is supported in part by the U. S. DOE under Contract No. DE-FG-02-85ER 40231.

- 
- [1] M. N. Achasov *et al.* (SND Collaboration), *Phys. Lett. B* **479**, 53 (2000); R. R. Akhmetshin *et al.* (CMD-2 Collaboration), *Phys. Lett. B* **462**, 380 (1999); A. Aloisio *et al.* (KLOE Collaboration), hep-ex/0107024; *Phys. Lett. B* **537**, 21 (2002); **536**, 209 (2002).
- [2] See the proceedings of the conferences: S. Ishida *et al.*, in *Proceedings of KEK, Soryushiron Kenkyu 102, 2000-4*, No. 5 (KEK, Tsukuba, 2000); D. Amelin and A. M. Zaitsev, in *Hadron Spectroscopy: Ninth International Conference on Hadron Spectroscopy HADRON 2001*, AIP Conf. Proc. No. 619 (AIP, New York, 2001); A. H. Fariborz, in *Scalar Mesons: an Interesting Puzzle for QCD, SUNY Institute of Technology, Utica, NY, 2003*, AIP Conf. Proc. No. 688 (AIP, New York, 2003).
- [3] N. N. Achasov and V. N. Ivanchenko, *Nucl. Phys.* **B315**, 465 (1989).
- [4] F. E. Close, N. Isgur, and S. Kumano, *Nucl. Phys.* **B389**, 513 (1993); N. N. Achasov and V. V. Gubin, *Phys. Rev. D* **56**, 4084 (1997); **57**, 1987 (1998); N. N. Achasov, V. V. Gubin, and V. I. Shevchenko, *Phys. Rev. D* **56**, 203 (1997); J. L. Lucio Martinez and M. Napsuciale, *Phys. Lett. B* **454**, 365 (1999); hep-ph/0001136; A. Bramon, R. Escribano, J. L. Lucio Martinez, M. Napsuciale, and G. Pancheri, *Phys. Lett. B* **494**, 221 (2000); Y. S. Kalashnikova, A. E. Kudryavtsev, A. V. Nefediev, C. Hanhart, and J. Haidenbauer, *Eur. Phys. J. A* **24**, 437 (2005).
- [5] S. Weinberg, *Phys. Rev. Lett.* **17**, 616 (1966).
- [6] D. Black, M. Harada, and J. Schechter, *Phys. Rev. Lett.* **88**, 181603 (2002). See also hep-ph/0306065 for some additional discussion.
- [7] M. Gell-Mann, D. Sharp, and W. G. Wagner, *Phys. Rev. Lett.* **8**, 261 (1962). A general formulation of the PVV interaction in a gauge invariant manner was given in T. Fujiwara, T. Kugo, H. Terao, S. Uehara, and K. Yamawaki, *Prog. Theor. Phys.* **73**, 926 (1985); O. Kaymakcalan, S. Rajeev, and J. Schechter, *Phys. Rev. D* **30**, 594 (1984); O. Kaymakcalan and J. Schechter, *Phys. Rev. D* **31**, 1109 (1985); P. Jain, R. Johnson, U. G. Meissner, N. W. Park, and J. Schechter, *Phys. Rev. D* **37**, 3252 (1988).
- [8] F. E. Close, N. Isgur, and S. Kumano, *Nucl. Phys.* **B389**, 513 (1993); J. E. Palomar, L. Roca, E. Oset, and M. J. Vicente Vacas, *Nucl. Phys.* **A729**, 743 (2003).
- [9] C. G. Callan, S. Coleman, J. Wess, and B. Zumino, *Phys. Rev.* **177**, 2247 (1969).
- [10] M. Harada and J. Schechter, *Phys. Rev. D* **54**, 3394 (1996).
- [11] D. Black, A. H. Fariborz, F. Sannino, and J. Schechter, *Phys. Rev. D* **59**, 074026 (1999).
- [12] M. Bando, T. Kugo, and K. Yamawaki, *Phys. Rep.* **164**, 217 (1988).
- [13] M. Harada and K. Yamawaki, *Phys. Rep.* **381**, 1 (2003).
- [14] O. Kaymakcalan, S. Rajeev, and J. Schechter, *Phys. Rev. D* **30**, 594 (1984); O. Kaymakcalan and J. Schechter, *Phys. Rev. D* **31**, 1109 (1985).
- [15] J. Schechter, *Phys. Rev. D* **34**, 868 (1986); K. Yamawaki, *Phys. Rev. D* **35**, 412 (1987); M. F. Golterman and N. D. Hari Dass, *Nucl. Phys.* **B277**, 739 (1986); U. G. Meissner and I. Zahed, *Z. Phys. A* **327**, 5 (1987).
- [16] A. M. Abdel-Rehim, D. Black, A. H. Fariborz, and J. Schechter, *Phys. Rev. D* **67**, 054001 (2003).
- [17] J. J. Sakurai, *Currents and Mesons* (Chicago University Press, Chicago, 1969). In the present context, see, for example, J. Schechter, *Phys. Rev. D* **34**, 868 (1986).
- [18] K. Kawarabayashi and M. Suzuki, *Phys. Rev. Lett.* **16**, 255 (1966); Riazuddin and Fayyazuddin, *Phys. Rev.* **147**, 1071 (1966).
- [19] M. Harada and K. Yamawaki, *Phys. Rev. Lett.* **87**, 152001 (2001). It was shown that this is also satisfied even at the quantum level in three flavor QCD.
- [20] S. Eidelman *et al.* (Particle Data Group), *Phys. Lett. B* **592**, 1 (2004) and 2005 Partial update for edition 2006 (<http://pdg.lbl.gov>).
- [21] A. H. Fariborz and J. Schechter, *Phys. Rev. D* **60**, 034002 (1999).

- [22] D. Black, A. H. Fariborz, and J. Schechter, Phys. Rev. D **61**, 074030 (2000).
- [23] See the result of the SND Collaboration in [1] above.
- [24] M. Harada, F. Sannino, and J. Schechter, Phys. Rev. D **54**, 1991 (1996).
- [25] M. N. Achasov *et al.*, Phys. Lett. B **485**, 349 (2000).
- [26] A. Aloisio *et al.* (KLOE Collaboration), Phys. Lett. B **537**, 21 (2002).
- [27] The A, B and C one loop form factors being used here were introduced in G. Passarino and M. Veltman, Nucl. Phys. **B160**, 151 (1979).
- [28] M. J. G. Veltman, Acta Phys. Pol. B **12**, 437 (1981); see also Ref. [13].
- [29] N. N. Achasov, Nucl. Phys. **A728**, 425 (2003).
- [30] N. N. Achasov, S. A. Devyanin, and G. N. Shestakov, Sov. J. Nucl. Phys. **32**, 566 (1980) [Yad. Fiz. **32**, 1098 (1980)]; Z. Phys. C **22**, 53 (1984); see also Ref. [41].
- [31] N. N. Achasov and A. V. Kisilev, hep-ph/0512047.
- [32] V. Cirigliano, G. Ecker, H. Neufeld, and A. Pich, J. High Energy Phys. 06 (2003) 012.
- [33] J. A. Oller, Nucl. Phys. **A727**, 353 (2003).
- [34] J. R. Pelaez, Mod. Phys. Lett. A **19**, 2879 (2004).
- [35] L. Maiani, F. Piccinini, A. D. Polosa, and V. Riquer, Phys. Rev. Lett. **93**, 212002 (2004).
- [36] R. L. Jaffe, Phys. Rev. D **15**, 267 (1977).
- [37] For a review see P. J. O'Donnell, Rev. Mod. Phys. **53**, 673 (1981).
- [38] D. Black, A. H. Fariborz, and J. Schechter, Phys. Rev. D **61**, 074001 (2000); D. Black, A. H. Fariborz, S. Moussa, S. Nasri, and J. Schechter, Phys. Rev. D **64**, 014031 (2001); T. Teshima, I. Kitamura, and N. Morisita, J. Phys. G **28**, 1391 (2002); **30**, 663 (2004); Nucl. Phys. **A759**, 131 (2005); F. E. Close and N. A. Tornqvist, J. Phys. G **28**, R249 (2002); A. H. Fariborz, Int. J. Mod. Phys. A **19**, 2095 (2004); M. Napsuciale and S. Rodriguez, Phys. Rev. D **70**, 094043 (2004); A. H. Fariborz, R. Jora, and J. Schechter, Phys. Rev. D **72**, 034001 (2005).
- [39] T. Teshima, I. Kitamura, and N. Morisita, J. Phys. G **28**, 1391 (2002).
- [40] A. Gokalp, A. Kuckarslan, S. Solmaz, and O. Yilmaz, J. Phys. G **28**, 2783 (2002); **28**, 3021(E) (2002).
- [41] N. N. Achasov and A. V. Kiselev, Phys. Rev. D **70**, 111901 (2004).
- [42] See the result of the KLOE Collaboration in [1] above.